



LAWRENCE  
LIVERMORE  
NATIONAL  
LABORATORY

# Incipient plasticity of single Crystal Tantalum as a function of temperature and orientation

O. Franke, J. Alcala, R. Dalmau, Z. C. Duan, J.  
Biener, M. M. Biener, A. M. Hodge

June 9, 2016

Philosophical Magazine

## **Disclaimer**

---

This document was prepared as an account of work sponsored by an agency of the United States government. Neither the United States government nor Lawrence Livermore National Security, LLC, nor any of their employees makes any warranty, expressed or implied, or assumes any legal liability or responsibility for the accuracy, completeness, or usefulness of any information, apparatus, product, or process disclosed, or represents that its use would not infringe privately owned rights. Reference herein to any specific commercial product, process, or service by trade name, trademark, manufacturer, or otherwise does not necessarily constitute or imply its endorsement, recommendation, or favoring by the United States government or Lawrence Livermore National Security, LLC. The views and opinions of authors expressed herein do not necessarily state or reflect those of the United States government or Lawrence Livermore National Security, LLC, and shall not be used for advertising or product endorsement purposes.

## Incipient plasticity of single Crystal Tantalum as a function of temperature and orientation

O. Franke<sup>1</sup>, Zhi Chao Duan<sup>1</sup>, J. Biener<sup>1,2</sup>, M.M. Biener<sup>2</sup>, J. Alcala<sup>3</sup>, Andrea M Hodge<sup>1</sup>

<sup>1</sup> *Department of Aerospace and Mechanical Engineering, University of Southern California, Los Angeles, 90089*

Nanoindentation data on Single-crystal Ta (100),(110),(111) are presented and the incipient plasticity or early stages of dislocations is studied statistically as a function of temperature and indentation rate. As a typical body centered cubic (bcc) metal, Tantalum revealed a unique deformation behavior, which was correlated to the dislocation theory and Peierls mechanism. Meanwhile, dislocation density and indentation tip size are also believed to affect the distributions of the load- displacement burst.

### 1. Introduction

The elastic-plastic transition during nanoindentation has been a hot topic in the past a few years focusing on a variety of materials []. Especially in well-prepared single crystals, the distinctive advantage of nanoindentation probing ultrasmall volumes allows these discontinuities in the load-displacement curves to be explained as the homogeneous nucleation of dislocations loops in the area of maximum stress underneath the indenter []. This is also the reason why the pop-in load is close to the theoretical strength of the material. Atomistic simulations on the other side proved that this assumption might not be true and that dislocations can be nucleated heterogeneously, as well []. ....

While in face centered cubic (f.c.c) system, the correlation between incipient plasticity and dislocation motion has been well understood [], in much more complex body center cubic (b.c.c) systems, despite of a few reports, there are still quite a few open questions. Most studies on the deformation behavior and the dislocation nucleation so far were carried out on nanopillars [] with a few studies using nanoindentation []. Schneider et al. showed that both orientation and the ratio of the test temperature to the critical temperature play an important role in the deformation behavior. While the orientation mostly affects the stress on the slip systems, the ratio of the test and critical temperature is a measure for the screw dislocation mobility, which is the limiting

factor in the deformation of BCC metals. At the critical temperature the mobility of screw dislocations reaches the level of edge dislocation mobility and the deformation behavior transitions to a serrated flow behavior[1]. However, prior studies varied the ratio of test and critical temperatures by selecting various materials and testing them at room temperature. In this study Ta was employed to advance the understanding of incipient plasticity in BCC materials but unlike in the other studies the temperature was increased to 200 °C which is beyond the critical temperature. The oxide formation during the experiments is limited to a layer of a few Angstroms on the surface and XPS of samples after heating showed no significant change in the oxide structure so that a contribution of the oxide in the measured pop-in load is not to be expected [2].

## 2. Experimental

Three low index Tantalum single crystals, Ta(100), Ta(110) and Ta(111) were prepared by a combination of electrochemical and mechanical polishing, resulting in a rms surface roughness below 1 nm. The crystallographic orientation of the samples was determined prior to cutting by Laue diffraction. All nanoindentation experiments were performed in the load-controlled mode using a commercial Hysitron Triboindenter (MN, USA) system. A Berkovich tip with a radius of curvature of ~190 nm was used to obtain quantitative load-displacement data, and a spherical tip with a tip radius of ~1 μm was also used for some of the tests as of comparison. Different loading rates of 1000 and 5000 μN/s were chosen both at room temperature and 200 °C. For nanoindentation experiments at 200 °C, the testing protocol described in an earlier paper [3] was followed. AFM imaging of the samples was carried out using a ... in the ... mode. The indents were imaged for both temperatures. The oxide structure and thickness were measured following the procedure described elsewhere [4].

### 3. Results

#### a) Orientation and rate dependence at room temperature

All three orientations exhibit a similar behavior at room temperature that manifests itself in a single pop-in event indicating the onset of plasticity. For none of the specimen serrated pop-ins were observed as they are usually encountered in fcc materials (e.g. Durst et al. Acta Mater. 54). Furthermore the pop-in displacement with several tens of nanometers is relatively large and relates to a significant number of dislocations being nucleated at the same time. Focusing on the low loading rate first it becomes obvious that the (111) orientation has the lowest pop-in load at ... equivalent to a contact pressure of ... GPa followed by the (110) oriented single crystal ( $P_{\text{pop-in}} = \dots$  and  $P_m = \dots$ ) and the (100) oriented single crystal ( $P_{\text{pop-in}} = \dots$  and  $P_m = \dots$ ). The same trend was observed for the loading rate dependence, which is almost non-existent for the (111) single crystal and increases successively over (110) and (100), where it is the most pronounced.

#### b) Elevated temperature

The deformation behavior of Ta changes markedly once the critical temperature of 177 °C is surpassed. Beyond this temperature cross-slip of screw dislocations is expected to contribute significantly to the total plastic deformation. This can be seen in the load displacement curves, where two discrete pop-ins, one at low loads and a second one at higher loads, for the (111) oriented Ta-single crystals. Both of the pop-ins are showing a significant pop-in displacement in the 10s of nanometers. So even though there is a nominally enhanced capability for plastic deformation, there is no significant sign for it to be found in the (111)-crystal. The transition is somewhat clearer in the (110) oriented specimen where at elevated temperatures above the critical temperature several pop-ins at various loads are observed with each of them yielding only

a few nanometers in displacement. This behavior is getting closer to the serrated flow observed in fcc-metals at low and high temperatures. Overall the most fcc-like behavior was found in the (100) sample that as described in the previous section was the one exhibiting the highest pop-in load and the biggest strain rate dependence at room temperature. Nonetheless, the load-displacement curves (Fig. xx) at 200 C are the most serrated (large numbers of relatively small displacement bursts).

In general the expected decrease of the pop-in load with increasing temperature was found, however it was found to be the most pronounced for the crystals that also undergo a change in their yielding behavior ((110) and (100)). In contrary to those two single for (111) the heating seems to have only a relatively mild influence on the mean contact pressure at which the onset of plastic flow occurs.

#### c) Loading rate effects at 200 C

The same two loading rates as at room temperature were used to study the effect of the loading rate at 200 C. However, there is no clear trend while (111) develops a small degree of loading rate dependence, the effect seems to be lost on (110) and unchanged for the (100) sample. The findings described above will be discussed in respect to the sample-orientation and the resulting screw dislocation mobility/stresses on the slip planes.

#### 4. Discussion

As described in the previous sections there is a significant influence of several factors on the incipient plasticity of bcc single crystals. However, the question remains if there is one uniting factor that can explain all these phenomena. The obvious approach is to look at the orientation first. Table 1 gives a summary of all the key findings and the relation of the surface normal to the slip planes. The contact can be considered Hertzian until the initial yielding shows as a

discontinuity in the load-displacement curve since the displacement at which the initial pop-in occurs is in the order of 10-20 % of the tip radius. As a consequence the sharp tip can be considered spherical for this study. Furthermore even though the stress state underneath the indenter is more complex than in a regular uniaxial tensile or compression test, the highest stress is expected directly underneath the center of the indenter (parallel to the surface normal) at a distance  $z = 0.48 a$  (where  $a$  is the contact radius). This is also the location where the initial yielding is expected to occur in compression along the loading direction. Based on those conditions the relation between surface normal and the slip planes is a useful indicator for the analysis of incipient plasticity. In particular in a system where a high degree of activation needs to be overcome due to the presence of the high Peierl's stresses.

Table 1: Orientation effects at room and elevated temperature

Single crystal orientation	Pop-in load at RT (LR = 1000 $\mu\text{N/s}$ )	Pop-in load at 200 °C (LR = 1000 $\mu\text{N/s}$ )	# of pop-in events RT/200 °C	Loading rate dependence RT/200 °C	Angle surface normal to [111] slip direction	Angle surface normal to (110) slip plane	Angle surface normal to (123) slip plane	Angle surface normal to (112) slip plane
(100)	+	o	1/+	+/+	54.7°	45°	74.5°	65.9°
(110)	o	o	1/o	o/o	35.3°	0°	55.5°	54.7°
(111)	-	-	1/2	-/o	0°	35.3°	22.2°	19.5°

(+ = high, o = medium, - = low)

By looking at the table it becomes evident that at room temperature the angle between slip system and loading direction is not a critical factor, which is most likely due to the low dislocation mobility in bccs. However, compression along the closest packed direction yields the lowest activation stresses for the onset of plastic deformation (independent of the orientation of the slip planes). Nonetheless it seems that for all room temperature seems to be limited to few active slip systems. This is also manifested in the AFM-images of the pile-up which show a squared geometry with xxx slip steps. Once the temperature is increased beyond the critical value (thus allowing for cross slip and enhancing the capability of the dislocations to overcome

the Peierl's stress by thermal activation), the orientation relationship of the highly compressed zone (compression occurs along the loading axis and thus parallel to the surface normal) and the slip planes plays a significant role. For instance the (100) single crystal with all slip planes being inclined towards the loading axis and the slip direction being almost at  $45^\circ$ , is also the one showing the most fcc-like behavior. This can be interpreted as a sign of significant slip on several slip planes at the same time. This observation does not only match with measured transition in the load-displacement curves but is also clearly visible in the AFM-images of the pile-up after elevated temperature indentation. There is an obvious change towards a more regular shaped pile-up. However, we would like to point out that the pile-ups are still representing the symmetry of the relevant plane, but the geometry of each pile-up is the feature that is changing of temperature.

In respect to the loading rate dependence the results are not as unambiguous as for the pop-in load itself. Still it seems as if orientations that depend on cross-slip and the activation of several slip systems (e.g. (100)) are more affected by the loading rate than materials that are deformed along either the closest packed plane (111) or a the closest packed direction (110). This could be taken as a sign that the screw dislocation mobility is still somewhat lower than the edge dislocation mobility (even at  $200^\circ\text{C}$ ), which would make the specimen requiring high quantities of screw dislocations to deform more susceptible to loading rate effects.

In conclusion it seems that once the thermal energy provided is sufficient to overcome the Peierl's stress materials the materials with high Schmid factors for several slip systems start deforming in a fcc-like manor.

## 5. Conclusion

In this paper, we have shown that there is a significant change in the deformation behaviour of a high-melting point BCC material (Ta) once the critical temperature is surpassed. The mean pop-in load increases from (1 1 1) to (1 1 0) and (1 0 0) which shows the highest resistance against localized yielding. A tentative explanation for the differences in the pop-in load of the three different orientations was found based on the stresses determined from FEM-modelling that showed that the high hydrostatic pressures encountered in indentation aid nucleating defects such as twins and SF. At 200 °C the (1 0 0)-oriented crystal shows a highly serrated P-h-curve. The serrated flow behaviour as found at 200 °C is an evolution of the defect networks due to the specific quasi-elastic reloading at a given orientation [10]. Analysis of the cumulative distributions of the critical load for all crystal orientations showed a strong effect due to temperature while the strain rate sensitivity was found to be minimal. Fluctuations and inconsistencies in the cumulative distributions were attributed to surface imperfections and additional defect mechanisms besides regular heterogeneous dislocation nucleation. MD simulations revealed the presence of higher energy mechanisms such as twinning and stacking fault generations which means that the MD simulations are the upper bound of the pop-in distribution [10], while the experiments in this study present the lower bound of the distribution. Furthermore, the secondary pop-ins were found to be a release mechanism of the stress accumulated in the quasi-elastic reloading after the initial yielding.

## 6. Acknowledgements

Parts of his work were performed under the auspices of the US Department of Energy at Lawrence Livermore National Laboratory under Contract DE-AC52-07NA27344.

## References

- [1] A.C. Lund, A.M. Hodge and C.A. Schuh, *Appl. Phys. Lett.* 85 (2004) p.1362.
- [2] J.K. Mason, A.C. Lund and C.A. Schuh, *Phys. Rev. B* 73 (2006) p.054102.
- [3] C.E. Packard, O. Franke, E.R. Homer and C.A. Schuh, *J. Mater. Res.* 25 (2010) p.2251.
- [4] C.A. Schuh and T.G. Nieh, *Acta Mater.* 51 (2003) p.87.
- [5] A. Barnoush, *Acta Mater.* 60 (2012) p.1268.
- Philosophical Magazine 11  
Downloaded by [Lawrence Livermore National Laboratory] at 12:20 14 November 2014
- [6] N. Gane and F.P. Bowden, *J. Appl. Phys.* 39 (1968) p.1432.
- [7] D.F. Bahr, S.L. Jennerjohn and D.J. Morris, *Jom-J. Min. Met. Mat. S* 61 (2009) p.56.
- [8] S. Akarapu, H.M. Zbib and D.F. Bahr, *Int. J. Plast.* 26 (2010) p.239.
- [9] A.A. Zbib and D.F. Bahr, *Metal. Mater. Trans. A* 38 (2007) p.2249.
- [10] J. Alcalá, R. Dalmau, O. Franke, M. Biener, J. Biener and A. Hodge, *Phys. Rev. Lett.* 109 (2012) p.075502.
- [11] A.B. Mann and J.B. Pethica, *MRS Online Proceedings Library* 436 (1996) p.153.
- [12] Z. Wang, H. Bei, E.P. George and G.M. Pharr, *Scripta Mater.* 65 (2011) p.469.
- [13] S.A.S. Asif and J.B. Pethica, *MRS Online Proceedings Library* 436 (1996) p.201.
- [14] D.F. Bahr, J.C. Nelson, N.I. Tymiak and W.W. Gerberich, *J. Mater. Res.* 12 (1997) p.3345.
- [15] W.W. Gerberich, J.C. Nelson, E.T. Lilleodden, P. Anderson and J.T. Wyrobek, *Acta Mater.* 44 (1996) p.3585.
- [16] M. Goeken and M. Kempf, *Zeitschrift fuer Metallkunde/Mater. Res. Adv. Tech.* 92 (2001) p.1061.
- [17] C. Begau, A. Hartmaier, E.P. George and G.M. Pharr, *Acta Mater.* 59 (2011) p.934.
- [18] H. Bei, Y.F. Gao, S. Shim, E.P. George and G.M. Pharr, *Phys. Rev. B: Condens. Matter Mater. Phys.* 77 (2008) p.060103.
- [19] D.-S. Xu, J.-P. Chang, J. Li, R. Yang, D. Li and S. Yip, *Mater. Sci. Eng. A* 387–389 (2004) p.840.
- [20] M.M. Biener, J. Biener, A.M. Hodge and A.V. Hamza, *Phys. Rev. B* 76 (2007) p.165422.
- [21] P. Engels, A. Ma and A. Hartmaier, *Int. J. Plast.* 38 (2012) p.159.
- [22] M.J. Cordill, N.R. Moody and W.W. Gerberich, *Int. J. Plast.* 25 (2009) p.281.
- [23] S. Brinckmann, J.-Y. Kim and J.R. Greer, *Phys. Rev. Lett.* 100 (2008) p.155502.
- [24] J.R. Greer, C.R. Weinberger and W. Cai, *Mater. Sci. Eng. A* 493 (2008) p.21.
- [25] J.-Y. Kim, D. Jang and J.R. Greer, *Acta Mater.* 58 (2010) p.2355.
- [26] S.W. Lee and W.D. Nix, *Philos. Mag.* 92 (2012) p.1238.
- [27] K.V. Rajulapati, M.M. Biener, J. Biener and A.M. Hodge, *Philos. Mag. Lett.* 90 (2010) p.35.
- [28] A.S. Schneider, B.G. Clark, C.P. Frick, P.A. Gruber and E. Arzt, *Mater. Sci. Eng. A* 508 (2009) p.241.
- [29] A.S. Schneider, C.P. Frick, B.G. Clark, P.A. Gruber and E. Arzt, *Mater. Sci. Eng. A* 528 (2011) p.1540.
- [30] J. Li, K.J. Van Vliet, T. Zhu, S. Yip and S. Suresh, *Nature* 418 (2002) p.307.
- [31] J.A. Moriarty, V. Vitek, V.V. Bulatov and S. Yip, *J. Comput. Aided Mater. Des.* 9 (2002) p.99.
- [32] C.S. Deo, D.J. Srolovitz, W. Cai and V.V. Bulatov, *J. Mech. Phys. Solids* 53 (2005) p.1223.
- [33] J.E. Dorn and A.K. Mukherje, *Trans. Metall. Soc. Aime* 245 (1969) p.1493.
- [34] S. Nemat-Nasser, T. Okinaka and L. Ni, *J. Mech. Phys. Solids* 46 (1998) p.1009.
- [35] S. Naka, A. Lasalmonie, P. Costa and L.P. Kubin, *Philos. Mag. A* 57 (1988) p.717.
- [36] G. Wang, A. Strachan, T. Çağın and W.A. Goddard, *Phys. Rev. B* 67 (2003) p.140101.
- [37] J. Marian, W. Cai and V.V. Bulatov, *Nat. Mater.* 3 (2004) p.158.
- [38] Z.C. Duan and A.M. Hodge, *Jom-J. Min. Met. Mat. S* 61 (2009) p.32.
- [39] Z.-L. Liu, X.-L. Zhang, L.-C. Cai, X.-R. Chen, Q. Wu and F.-Q. Jing, *J. Phys. Chem. Solids* 69 (2008) p.2833.
- [40] J. Alcalá, O. Casals and J. Ocenásek, *J. Mech. Phys. Solids* 56 (2008) p.3277.

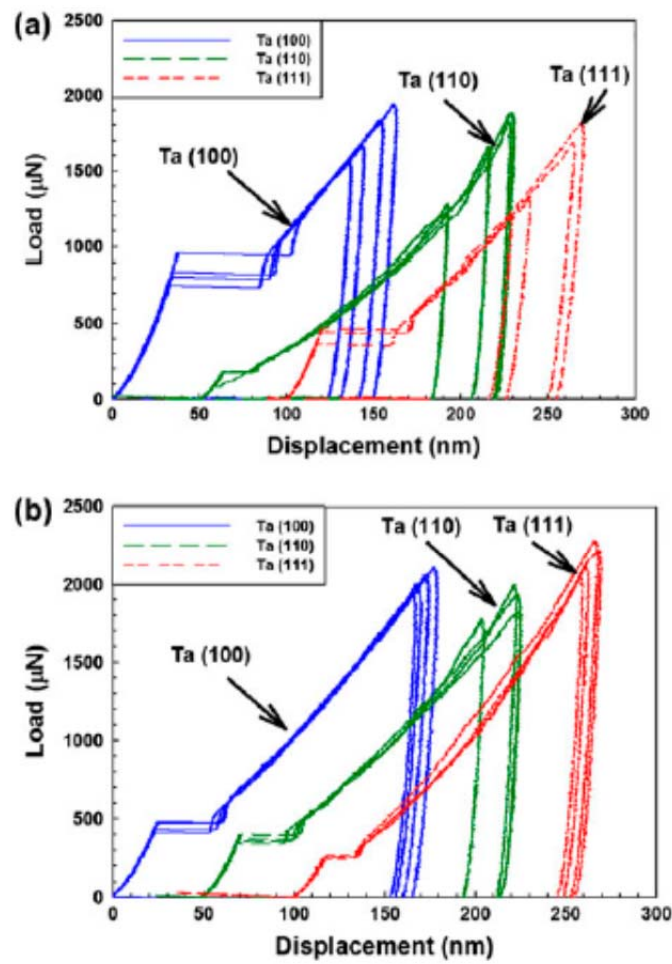


Figure 1. (colour online) Representative room temperature load-displacement (P-h) curves for (1 0 0), (1 1 0) and (1 1 1) Ta single crystals at a loading rate of (a) 1,000  $\mu\text{N/s}$  and (b) 5,000  $\mu\text{N/s}$ . Curves are offset for viewing purposes.

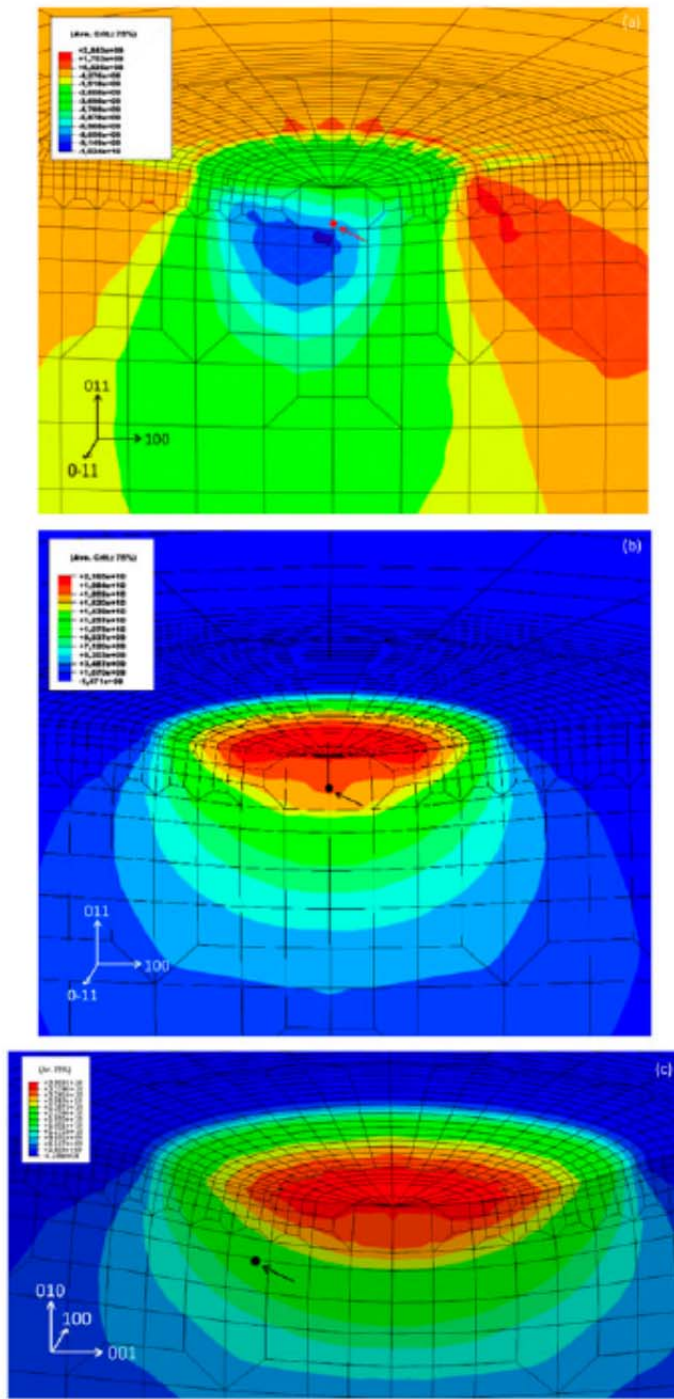


Figure 2. (colour online) Stress fields at the imposed ratio between contact radius and indenter diameter,  $a/D$ , leading to defect nucleation. The approximate locations of defect nucleation are marked with arrows. Part (a) gives the isocontours of shear stress in  $(110)$  indentation for the planes and directions where the twin in Figure 2(b) nucleates. Part (b) gives the isocontours of hydrostatic pressure associated with Part (a). Part (c) provides the isocontours of hydrostatic pressure at the onset where a  $(011)$  stacking fault nucleates in  $(100)$  indentation [10].

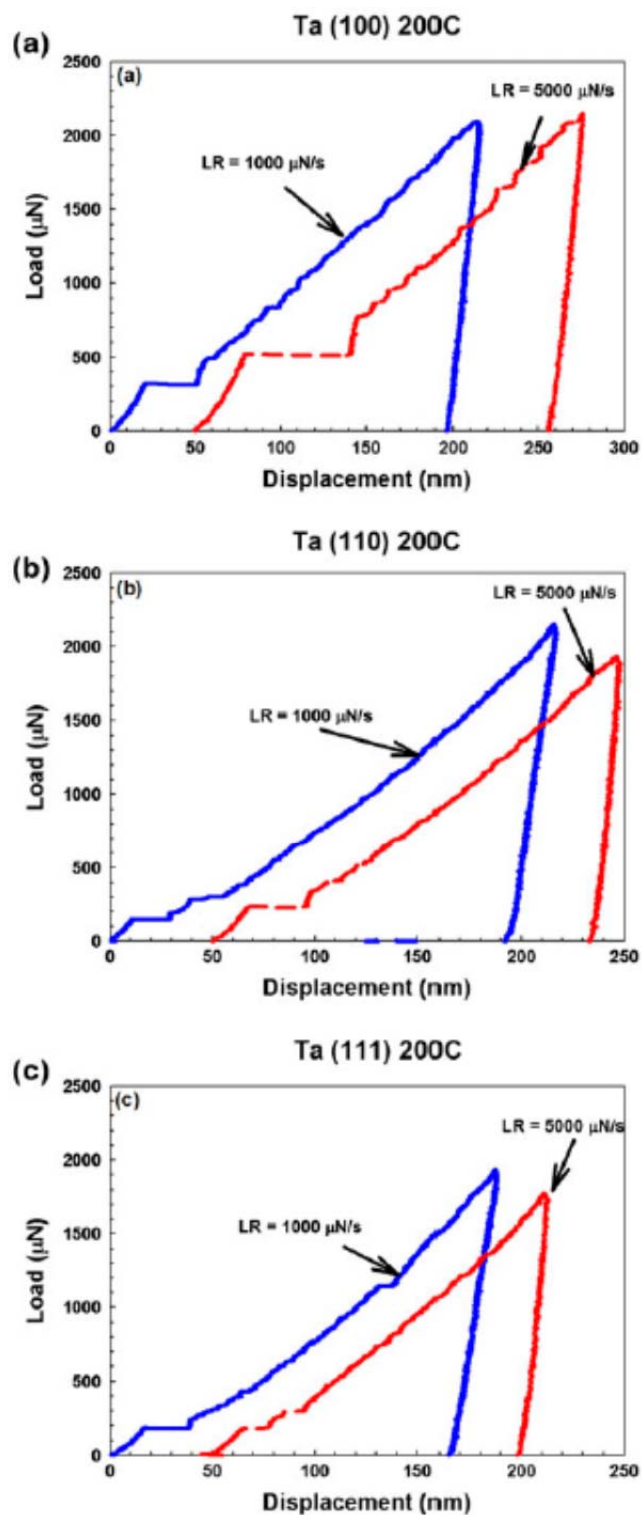


Figure 3. (colour online) (a) Representative load-displacement (P-h) curves at 200 °C for loading rates of 1,000 and 5,000  $\mu\text{N/s}$  for three different Ta crystal orientations (a) (1 0 0), (b) (1 1 0) and (c) (1 1 1). Curves are offset for viewing purposes.

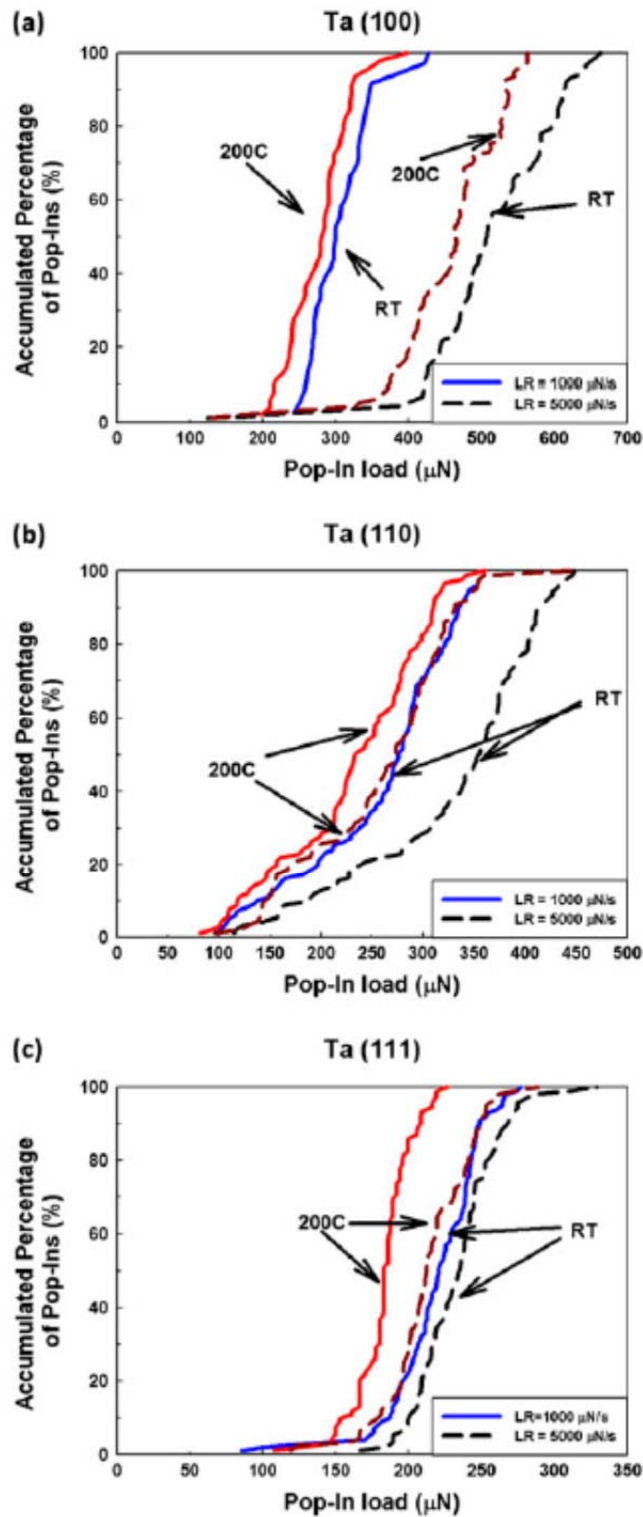


Figure 4. (colour online) Normalized cumulative distributions of the critical load at room temperature and at 200 °C for loading rates of 1,000 and 5,000  $\mu\text{N/s}$  for the three different Ta crystal orientations: (a) (1 0 0), (b) (1 1 0) and (c) (1 1 1).